Eur. Phys. J. D **41**, 505–511 (2007)
DOI: 10.1140/epjd/e2006-00270-4

THE EUROPEAN PHYSICAL JOURNAL D

Electronic excitations during grazing scattering of hydrogen atoms on KI(001) and LiF(001) surfaces

S. Lederer[1], H. Winter[1,a], HP. Winter[2], and F. Aumayr[2]

[1] Institut für Physik der Humboldt-Universität zu Berlin, Brook-Taylor-Str. 6, 12489 Berlin-Adlershof, Germany
[2] Institut für Allgemeine Physik der Technischen Universität Wien, Wiedner Hauptstr. 8 - 10, 1040 Wien, Austria

Received 23 June 2006 / Received in final form 3 November 2006
Published online 13 December 2006 –

Abstract. The energy loss of hydrogen atoms with energies of 400 eV and 1 keV is studied in coincidence with the number of emitted electrons during grazing scattering from atomically clean and flat KI(001) and LiF(001) surfaces. The energy loss spectra for specific numbers of emitted electrons are analyzed in terms of a binary interaction model based on the formation of transient negative ions via local capture of valence band electrons from anion sites. Based on computer simulations we derive for this interaction scenario probabilities for the production of surface excitons, for electron loss to the conduction band of KI, for emission of electrons, and for formation of negative hydrogen ions. The pronounced differences of data obtained for the two surfaces are attributed to the different electronic structures of KI and LiF.

PACS. 79.20.Rf Atomic, molecular, and ion beam impact and interactions with surfaces – 79.60.Bm Clean metal, semiconductor, and insulator surfaces

1 Introduction

It is known for a long time that electron emission is very efficient for impact of atomic particles on insulator surfaces [1]. As prominent example, we mention total electron yields observed for ionic crystals which in general clearly exceed those for metal targets [2,3]. Since occupied electronic levels in ionic crystals have higher binding energies (typically 10 eV) compared to the work function of a clean metal target (about 4 to 5 eV), this finding is at first glance surprising. In an early interpretation, this feature was partly explained by larger electron transport length within the bulk of insulators owing to the wide electronic band gap of these materials. In recent years, detailed investigations on the scattering of fast atoms and ions from alkali halide and oxide surfaces have been performed by a number of groups and revealed new details on the interaction mechanisms [4–8]. In summarizing those studies, it turns out that for projectiles with velocities below 1 a.u. (1 a.u. = v_0 = Bohr velocity) the formation of negative ions plays a key role for the interaction of atomic particles with ionic crystals. Evidence for this mechanism was first obtained from the observation of large fractions of negative ions in the scattered beams which can amount in specific cases close to 100 percent [6,7]. This effect was attributed to a local capture of electrons from anion sites which form the flat valence band of the crystal. The confluence of levels during this process is mediated by the Madelung potential for a site active in charge transfer acting on the affinity level of the negatively charged projectile ion [9,10]. Then the energy defect in those binary collisions is substantially reduced resulting in considerable probabilities for electron transfer and for the formation of negative ions. By recording the projectile energy loss in coincidence with electrons emitted during grazing scattering of 600 eV protons from a LiF(001) surface, Roncin and coworkers [11] identified the population of surface excitons as important excitation channel. In similar studies using hydrogen atoms over a wide energy range and measurements of negative ion fractions for the scattered beam, a detailed analysis was recently performed by us and provided an effective microscopic description for the complex interaction scenario [12–14].

For a LiF(001) surface, three steps dominate the electronic excitation process: (1) formation of a negative ion via electron capture from a F($2p$) lattice ion, (2) population of a surface exciton or escape of a negative ion from an active site, (3) detachment of negative ions under emission of electrons. This interaction sequence is repeated during the passage of further lattice sites over complete trajectories. For scattering under a glancing angle Φ_{in} of typically 1°, the number of effective collisions n_{coll} amounts to about 10. For the initial capture event the energy defect plays an important role, since this quantity determines the probability for the negative ion formation. This is evident from experiments on the formation of negative ions using different alkali halide surfaces, where for targets with lower

[a] e-mail: winter@physik.hu-berlin.de

binding energies of valence band electrons E_{bind} a substantial increase in the negative ion fractions is observed for elements with higher electron affinity (e.g., O, Cl, or F) [7]. It turns out, however, that for the formation of H^- ions the reduction of E_{bind} from about 12 eV for F($2p$) in LiF(001) to 8 eV for I($5p$) in KI(001) does not lead to the expected increase for the H^- fractions. This was attributed to direct electron loss to the conduction band owing to the different energy of the bottom of the band for KI compared to LiF. The work presented here was motivated by the issue to understand this electron loss in more detail. We have performed experiments with a KI(001) mono-crystalline surface and recorded all excitation and interaction products during complete grazing scattering events of atomic hydrogen atoms. From the detection of the energy loss of scattered projectiles in coincidence with the number of emitted electrons and measurements of H^- fractions, we are able to quantify contributions from the relevant electronic excitation channels within the framework of a probability approach in computer simulations. We reveal that electron loss to the conduction band plays indeed an important role for KI(001), whereas this contribution can be neglected for scattering from LiF(001) [14,15].

2 Model for electronic excitations during scattering from surfaces of ionic crystals

In recent years a detailed understanding for the electronic excitations during grazing scattering from surfaces of ionic crystals has been achieved. The transient formation of negative ions and the wide band gap of the target are important features of the interaction during the atom-surface collision. Grazing scattering proceeds in the regime of surface channeling where atomic projectiles are steered in terms of small angle scattering from the topmost layer of surface atoms ("surface channeling") [16,17]. In this regime of scattering, projectiles are specularly reflected from the surface on well defined trajectories passing over a fair number of lattice sites of the crystal. Interactions with the surface proceed in a sequence of defined charge transfer and excitation events. In Figure 1 we show a sketch of the interaction mechanisms for the scattering of a hydrogen atom from the surface of an ionic crystal. The energy diagram shown holds for the case of KI. The interaction cycle starts with electron capture of an electron from an anion site (here: I^-) where the confluence of levels for the efficient formation of the negative ions is mediated by the Madelung potential of the adjacent point charge lattice [9,10]. The energy defect ΔE between initial ($H^\circ + I^-$) and final ($H^- + I^\circ$) potential curves determines the probability for an electronic transition P_{bin}. In previous studies with LiF(001) we have shown that this probability can be approximated by the Demkov approach [18,19]

$$P_{bin} = \frac{1}{2}\ \mathrm{sech}^2\left(\frac{\pi\alpha\Delta E}{2v}\right) \qquad (1)$$

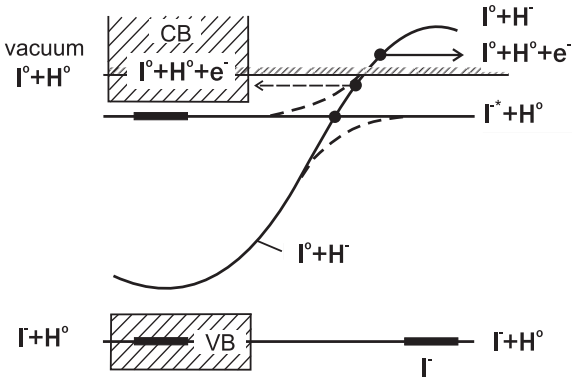

Fig. 1. Sketch of potential energy curves for illustration of interaction mechanisms during grazing scattering of hydrogen atoms from KI surface (for details see text).

with α being the decay length of the coupling and v the projectile velocity. P_{bin} increases for smaller energy defects ΔE and increasing velocity. Since the minimum of binding energies for valence electrons of KI (8 eV) is clearly smaller than for LiF (12 eV), we expect substantially higher P_{bin} for interactions with KI surfaces compared to LiF (see below). During escape from the active site after charge transfer, the shifted H^- level will cross the surface exciton level, a localized electron-hole pair excitation of the anion. The chance for population of an exciton $(1 - P_{LZ})$ can be derived from Landau-Zener theory [19] from the probability P_{LZ} for staying on the ($H^- + I^\circ$) potential curve during crossing with ($H^\circ + I^{-*}$). After survival from this crossing of potential energy curves, an H^- ion can lose its electron to unoccupied states of the conduction band via a resonant electron tunneling process.

It is important here that the conduction band of KI begins closely above the exciton level at about 2 eV below vacuum energies, whereas for LiF the band gap of 14 eV extends to about 2 eV above vacuum. Whereas for the analysis of the interaction scenario for LiF electron loss to the conduction band turns out to play a minor role, we will show below that the data obtained for the KI(001) surface can only be understood by taking into account a considerable probability P_{CB} for transitions from the H^- level to unoccupied states of the valence band of KI. Fractions of H^- ions which have survived electron loss to exciton and conduction band states may detach with probability P_{det} during interactions at adjacent lattice sites. Negative ions which have overcome detachment will affect the interaction sequence in a specific manner (see also reaction scheme in Fig. 2) and will lead in the final part of the scattering event to H^- ions found in the scattered beam.

In Figure 2 we display a schematic diagram for the interaction sequence starting with an incident neutral atom which undergoes with probability P_{bin} a transition to form a H^- ion. With probability $(1 - P_{bin})$ no charge transfer takes place, and the next chance for electron capture will occur during passage of the following anion site. During escape from the site active in electron transfer, the transient negative ion state has a probability P_{LZ} to survive the crossing with the exciton level. With probability

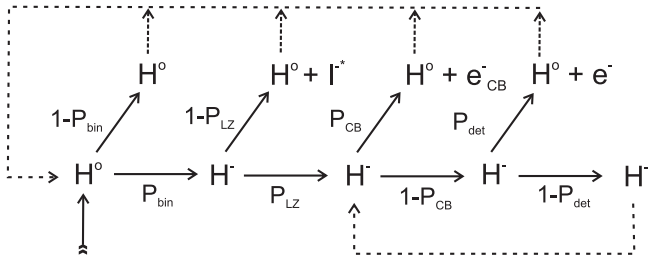

Fig. 2. Reaction scheme for illustration of interaction mechanisms during grazing scattering of hydrogen atoms from KI surface (for details see text).

$(1-P_{LZ})$ a surface exciton is produced, and the projectile continues the scattering process as neutral atom. Electron loss to the conduction band with probability P_{CB} will result in a detachment of the H^- ion.

In addition, other mechanisms of ion detachment (collisions with adjacent lattice atoms, resonant coherent ionization owing to the periodic potential of the point charge lattice of the crystal, etc. [6–8,20] with an overall probability P_{det} may occur. The separation of these two different processes for detachment is chosen here, since their outcome has a substantial effect on electron emission. Electrons excited to the conduction band with probability P_{CB} will not contribute to electron emission. In the final part of the interaction sequence H^- ions have a probability $P_{surv} = (1-P_{CB})\ (1-P_{det})$ to survive from detachment. We note that those fractions of surviving H^- ions can not undergo electron capture or populate surface excitons and are "trapped" in the detachment circle during collisions with further lattice atoms with probability P_{surv}.

In our work on scattering of atoms from LiF(001) we have initially described the data in terms of an analysis based on concepts of binomial statistics. The complex interaction scenario as sketched in Figures 1 and 2 indicates, however, that it is hardly possible to model the sequence of collisions in a closed analytical form. We therefore analyzed our data in terms of Monte-Carlo simulations where the collision sequence is followed over complete trajectories. For a modelling of the complete scattering event, all probabilities in the reaction scheme have to be known as function of distance from lattice sites and projectile velocity. This implies calculations of the relevant potential curves which are not available at present. We therefore perform an effective description of the atom-surface collisions. A mean interaction length, i.e. an effective number of collisions n_{coll} enters the computer simulations, where probabilities P_{bin}, P_{LZ}, P_{CB}, and P_{det} are free parameters. It turns out that the experimentally observed electronic excitation channels as well as the final H^- fractions can be reproduced fairly well by a reasonable choice of parameters.

3 Experiment and results

The experiments were performed in an UHV scattering chamber at a base pressure of 3×10^{-11} mbar. A well collimated beam of protons with energies of 400 eV and 1 keV is chopped by a pair of electric field plates with a voltage of some 10 V and rise times of some ns and is thereafter neutralized in a gas target operated with Kr gas. The neutral atoms are scattered under grazing angles of incidence Φ_{in} between about 1° and 2° from the clean and flat LiF(001) and KI(001) surface. The target surface is prepared by cycles of grazing sputtering with 25 keV Ar^+ ions and subsequent annealing at about 270 °C. During the experiments the target is kept on a temperature of about 100 °C, in order to avoid effects of macroscopic charging of the target on low energy electrons. The motion of projectiles parallel to the surface proceeds with energy $E_{\|} = E\cos^2(\Phi_{in}) \approx E$, the normal motion with $E_z = E\sin^2(\Phi_{in})$. Trajectory lengths scale as $s = z/\sin(\Phi_{in}) \approx v_z t/\Phi_{in} \sim 1/\Phi_{in}$ for a constant normal velocity $v_z = v\sin(\Phi_{in})$ [17]. Specularly reflected projectiles are detected 1.28 m behind the target by means of a channelplate detector which provides the "start" signal for our time-of-flight (TOF) setup. The overall time resolution in our experiments is typically 1 to 2 ns and is determined by the chopping of the incident ion beam and the stability of the electronic delay for the chopper signal. For the projectile beam the full width at half maximum (FWHM) of the TOF spectra is 8.6 ns (400 eV) and 7.5 ns (1 keV) which is equivalent to an energy resolution of 2.2 eV at a projectile energy of 400 eV and 4.4 eV at 1 keV. TOF spectra are recorded in coincidence with the pulse height of a surface barrier detector (SBD, pulse height ∼ number of emitted electrons) biased at a voltage of 25 keV [21]. A highly transparent grid of about 98 percent transmission on a voltage of some 10 eV is used to collect emitted electrons. This method of detection allows us to obtain information on the relevant elastic and inelastic interaction events (for details see Ref. [14]). TOF events coincident with the noise signal of the SBD are attributed to processes without emission of an electron. With a pair of electric field plates behind the target and a second channeltron detector we analyzed the charge fractions of the scattered beam and obtained the fractions of H^- ions n_{min}.

As example for the coincident detection of TOF and electron emission events, we have plotted in Figure 3 a 2D-spectrum (time of flight vs. SBD pulse height) recorded during scattering of 400 eV hydrogen atoms from a KI(001) surface under $\Phi_{in} = 1.8°$. Similar as in previous work with a LiF target [11–14] a number of discrete peaks can be identified in the spectrum. It is straightforward to ascribe the peak with very small energy loss and related to events without electron emission to elastically scattered projectiles (peak in lower left corner of plot in Fig. 3). The transfer of projectile energy to the crystal in terms of elastic binary collisions with lattice atoms is negligibly small for our scattering conditions [22]. The further peaks observed without electron emission stem from excitations of surface excitons [11]. The peaks found for higher pulse heights of the SBD are related to the emission of one electron and additional populations of surface excitons.

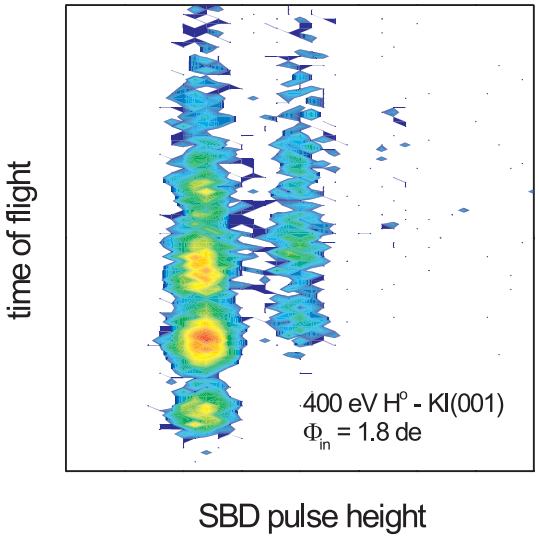

Fig. 3. (Color online) TOF – SBD pulse height representation of coincident data for scattering of 400 eV H° atoms from KI(001) under $\Phi_{in} = 1.8°$. 2D-plot shows raw data. Left column from bottom to top: events related to emission of no electron (elastic scattering, production of one, two, etc. excitons), next column from bottom to top: events related to emission of one electron without and with production of one, two, etc. excitons.

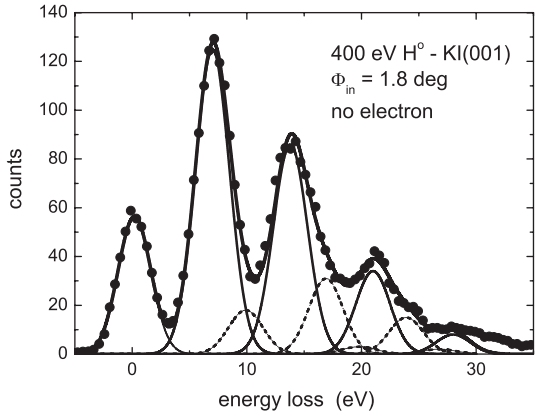

Fig. 4. Energy loss spectrum coincident with emission of no electron for scattering of 400 eV H° atoms from KI(001) under $\Phi_{in} = 1.8°$. Full circles: experiment, solid curves: fit to data with Gaussian line shape. Thin solid curves: elastically scattered projectiles and production of surface excitons; dashed curves: electron loss to conduction band.

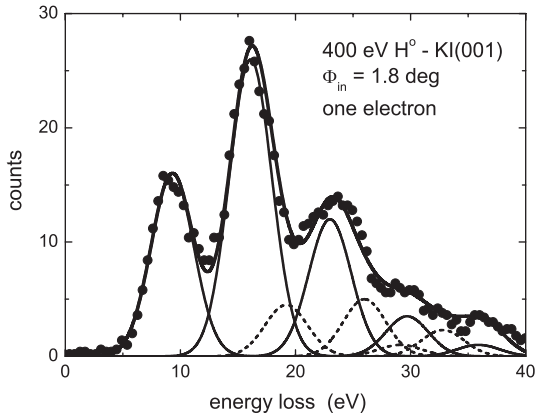

Fig. 5. Same as Figure 4, but spectrum coincident with emission of one electron.

For a more detailed analysis, we select events with SBD pulse heights equivalent to the noise of the detector (no electron emission) and project the data onto the TOF axis. After transformation to an energy scale we obtain the energy loss spectrum displayed in Figure 4. The solid curve is a best fit to a number of discrete peaks with Gaussian line shapes of constant FWHM of 3.5 eV. Similar as for scattering of H atoms from LiF we observe prominent peaks which are ascribed to elastic scattering (energy loss $\approx$ 0 eV) and population of discrete numbers of surface excitons. The excitation energies obtained from the fit are multiples of 6.8 eV; this is clearly less than 12 eV observed for LiF [7,11–14].

A closer inspection of the spectrum, however, indicates that additional components are present. The dashed curves in Figure 4 represent additional peaks with the same line width which lead to a perfect reproduction of the measured spectrum. These additional structures can consistently be understood by electron loss of H^- ions to the conduction band of KI. The small peak at an energy loss of 9.5 eV is attributed to loss of one electron, the more prominent peak at 16.3 eV (6.8 eV + 9.5 eV) to production of one exciton and loss of one electron, and at 19.0 eV we find an indication for loss of two electrons to the conduction band. The peak at 23.1 eV (13.6 eV + 9.5 eV) stems from the production of two excitons and loss of one electron.

The time and energy resolution of our setup does not allow us to perform studies with higher resolution on these peak structures. However, the values for the discrete energy losses are fairly consistent with the established electronic structure of KI. From the excitation energy of the surface exciton (5.9 eV) [23] we conclude that the majority of electrons is excited from about 1 eV below the top of the valence band. This is also consistent with the binding energy of 8.2 eV [24] for the top of the valence band, since the emission of electrons and the excitation to the conduction band is observed at energies slightly above 9 eV. At higher projectile energies, the energy resolution gradually decreases and does not allow us to resolve peak structures in the energy loss spectra (see spectra for projectile energy of 1 keV shown in Fig. 8).

In Figure 5 we display from the data in Figure 3 the energy loss spectrum for the emission of one electron. The peak at an energy loss of 9.3 eV is attributed to the excitation of a valence band electron to vacuum energies and subsequent emission via detachment of the negative ion. We note that this energy loss is slightly less than 9.5 eV as observed for the electron loss to the conduction band. The subsequent peaks in the spectrum can be ascribed, similar as for the emission of no electron, to the additional production of surface excitons and excitation to the conduction band. With a slightly larger FWHM of 4.2 eV we

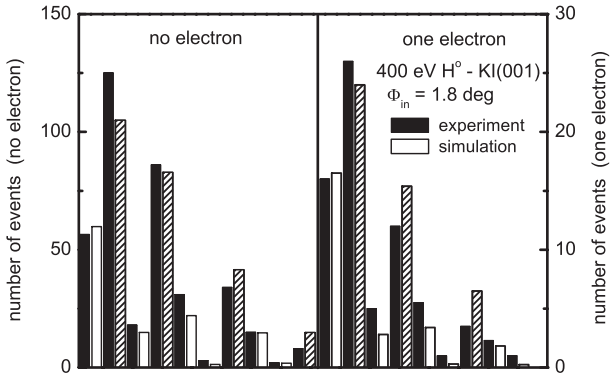

Fig. 6. Bar graphs for energy loss channels during scattering of 400 eV H° atoms from KI(001) surface under $\Phi_{in} = 1.8°$, ordered as measured energy loss peaks shown in Figures 4 and 5. Left panel: no electron emitted, right panel: one electron emitted. Full bars: experiment, open and hatched (production of excitons) bars: results from simulation.

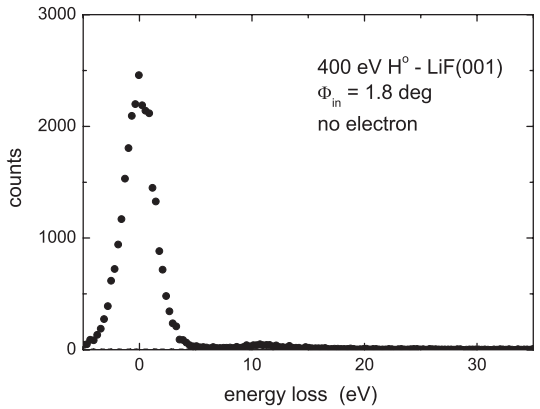

Fig. 7. Energy loss spectrum coincident with emission of no electron for scattering of 400 eV H° atoms from LiF(001) surface under $\Phi_{in} = 1.8°$.

can fit the data of this spectrum fairly well. Note that also here contributions of electron loss to the conduction band have to be incorporated in order to reproduce the spectrum.

From the spectra shown in Figures 4 and 5 we obtain the contributions of the relevant interaction channels and plot in Figure 6 their probabilities normalized to an arbitrarily chosen number of events. The left panel contains events without emission of an electron, the right panel events related to the emission of one electron (note that the scale of the right panel is enlarged by a factor of 5). The full bars are results from the experiment, the open and hatched bars represent results from our simulations where hatched bars indicate additional excitations of excitons only. Based on trajectory calculations and the lattice constant of the KI crystal ($a = 13.2$ a.u.) we have chosen an effective number of collisions $n_{coll} = 12$. Reasonable agreement with the distribution of reaction products shown in Figure 6 is achieved with $P_{bin} = 0.16$, $P_{LZ} = 0.22$, $P_{CB} = 0.3$, $P_{det} = 0.3$.

In view of our effective approach we consider these parameters as first estimates for the relevant interaction parameters. A more detailed analysis can only be performed in terms of theoretical treatments where the pronounced dependences of the relevant parameters on the distance from the surface is taken into account over the full trajectory. We note that the parameters given reproduce the experimental total electron yield $\gamma = 0.170$ and the H^- fractions in the scattered beam of about 4 percent. From our simulations we find that $P_{elast} = 7.8$ percent of the projectiles are elastically scattered and that $P_{el} = 9.5$ percent of the electronic excitations end up in the emission of an electron. The majority of excitation goes with $P_{ex} = 73$ percent into the excitonic branch, whereas electron loss to the conduction band is only $P_{CB} = 10$ percent. These small contributions, however, have to be taken into account in order to reproduce details of the energy loss spectra (cf. Figs. 4 and 5).

The majority of studies on grazing scattering from alkali halide surfaces were performed with LiF(001) [6–8,11–15]. For LiF crystals, valence band electrons have binding energies $E_{bind} > 12$ eV which is about 4 eV larger than for KI(001). As already worked out in detailed studies on the formation of negative ions [7], the energy gap and the resulting P_{bin} are clearly larger for LiF compared to KCl or KI. This feature is demonstrated in Figure 7 by an energy loss spectrum for scattering from a LiF(001) surface under otherwise same conditions (400 eV H°, $\Phi_{in} = 1.8°$). We reveal that almost the complete beam is scattered elastically from the LiF surface without electronic excitation or electron emission. The probability for production of a surface exciton is only 2 percent, and the total electron yield amounts to $\gamma = 3 \times 10^{-3}$. Therefore the probability for capture of a valence band electron is $P_{bin} \approx 0.0025$, almost two orders of magnitude smaller than for KI. The data are reproduced assuming $n_{coll} \approx 10$ collisions, $P_{LZ} = 0.2$, and $P_{det} = 0.25$ (see also former work on this topic [7,11–15]). The slightly smaller n_{coll} for scattering from LiF(001) compared to KI(001) is attributed to the stronger planar potential for scattering of hydrogen atoms from these surfaces. It is interesting to note here that, irrespective of the vast difference in the probabilities for electron capture, the H^- fractions are almost comparable for scattering from the two surfaces ($n_{min} \approx 1.5 \times 10^{-3}$ for LiF, $n_{min} \approx 4 \times 10^{-3}$ for KI). We ascribe this feature primarily to the additional detachment of H^- ions via electron loss to the conduction band (cf. Figs. 1 and 2).

The primary capture process is characterized by an energy defect ΔE in the collision which is evident from the expression for P_{bin} in equation (1). As has been demonstrated in previous studies with LiF [12–15], P_{bin} shows a pronounced increase with projectile velocity (energy). It is therefore of interest to investigate how for KI the outcome of scattering for enhanced P_{bin} is affected by electron loss to the conduction band. In Figure 8 we show for 1 keV H° projectiles energy loss spectra coincident with the emission of no electron (open circles), one electron (full circles), and three electrons (open squares). The angle of incidence

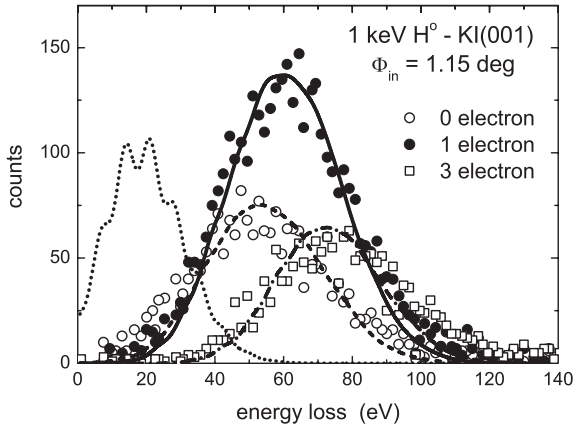

Fig. 8. Energy loss spectrum coincident with emission of no electron (open circles), one electron (full circles), three electrons (open squares) for scattering of 1 keV H° atoms from KI(001) under $\Phi_{in} = 1.15°$. Solid (one electron), dashed (no electron), dashed dotted (three electrons) curves: result of simulations. Dotted curves: simulation under neglect of electron loss to conduction band ($P_{CB} = 0$).

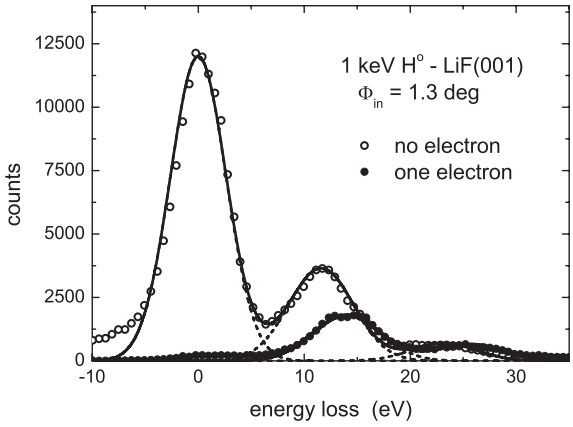

Fig. 9. Energy loss spectrum coincident with emission of no (open circles) and one (full circles) electron for scattering of 1 keV H° atoms from LiF(001) under $\Phi_{in} = 1.3°$. Solid and dashed curves: fit to data with Gaussian line shape.

is chosen to $\Phi_{in} = 1.15°$ in order to match closely the same energy for the motion normal to the surface $E_z \approx 0.5$ eV as for the 400 eV H° atoms. Then the distance of closest approach of trajectories to the surface plane are the same in both cases, and effective trajectory lengths scale as $1/\Phi_{in}$. The substantial energy loss of typically 50 eV and a total electron yield $\gamma = 1.7$ are clear signatures for an enhanced capture probability P_{bin}. This is also the conclusion from our analysis, however, the details of the interaction sequence are more intricate.

The curves in Figure 8 show results from our simulations with the interaction scheme outlined above. Striking feature of this work is the finding that the spectra can only be reproduced, if the electron loss to the conduction band is taken into account. This is demonstrated by the dotted curve in the figure which represents the energy loss spectrum (one electron emitted) for an evaluation as performed in previous work with LiF, i.e. neglect of electron loss to the conduction band. We note that for this case the electron number distribution and the experimental total electron yield are well described by $P_{bin} = 0.3$ and $P_{LZ} = 0.4$, but the calculated energy loss spectrum (dotted curve) is in disagreement with the experiment. From this result it is evident that electron loss to the conduction band has to be taken into account for the description of the electronic excitation processes.

A direct consequence of a nonzero P_{CB} is a larger P_{bin} in order to compensate the electron loss for the electron emission channel. Fair agreement between simulated and experimental energy loss spectra is obtained by enhancing the probability for initial capture to $P_{bin} = 0.42$ and for electron loss to $P_{CB} = 0.4$. For $n_{coll} = 20$ we have furthermore $P_{LZ} = 0.39$ and $P_{det} = 0.7$. The full circles in Figure 8 represent the energy loss spectrum coincident with the emission of one electron which is well reproduced by the set of parameters chosen (solid curve). Note that all spectra are plotted with respect to the same scale, i.e. events with emission of one electron are most abundant. The total electron yield is $\gamma = 1.7$. The open circles and open squares are data coincident with the emission of no electron and three electrons, respectively. Both spectra are also well reproduced within the same simulation (dashed curve for spectrum coincident with no electron emitted, dashed dotted curve with emission of three electrons). In our simulations we derive a negative ion fraction $n_{min} = 3.5$ percent and $\gamma = 1.6$ which is in good agreement with the experimental values $n_{min} = 4.5$ percent [25] and $\gamma = 1.7$. Furthermore we reveal from our calculations that only a negligible fraction of 2.6×10^{-5} undergoes elastic scattering. 42 percent of all events lead to population of surface excitons, 26 percent to excitation to the conduction band, and 32 percent to electron emission.

The electronic structure of LiF(001) shows a minimum binding energy for F($2p$) electrons of about $E_{bind} \approx 12$ eV and a band gap of $E_g \approx 14$ eV which extends about 2 eV into vacuum energy [24]. Therefore the energy defect in the primary collision is larger and P_{bin} is expected to be smaller compared to KI. Furthermore, previous studies have shown that, owing to the position of the conduction band, electron loss to this band seems to play a minor role for scattering from LiF.

In Figure 9 we display energy loss spectra for the scattering of 1 keV H° atoms from LiF(001) under $\Phi_{in} = 1.3°$. The dominance of the peak for elastically scattered projectiles indicates that the capture probability P_{bin} has to be clearly smaller than for scattering from KI (cf. Fig. 8). The spectra shown in Figure 9 can be described by the parameters $n_{coll} = 10$ collisions, $P_{bin} = 0.045$, $P_{LZ} = 0.3$, and $P_{det} = 0.4$. With these numbers we derive a negative ion fraction $n_{min} = 0.02$ and a total electron yield $\gamma = 0.12$ which compare well with the experiment. For the interaction scenario (neglect of electron loss to the conduction band, i.e. $P_{CB} = 0$) we reveal that 60 percent of all scattering events proceed elastically, whereas 29 percent end up in production of surface excitons and

11 percent in the emission of an electron. These examples show that electronic excitation and electron emission during scattering of H° atoms from KI and LiF surfaces are clearly different. In view of this fact, it is interesting to note that the H^- fractions of the scattered beams are about the same for a projectile energy of 1 keV, whereas the electron yields differ by a factor of about 10. Based on our simulations we explain this finding by the important role of the conduction band of KI for additional electron loss in the collision sequence.

4 Conclusions

We have presented detailed studies on electronic emission and excitation phenomena for grazing impact of neutral hydrogen atoms with energies of 400 eV and 1 keV on a KI(001) and LiF(001) surface. From measurements of fractions of emitted electrons, population of surface excitons and conduction band states as well as negative ion fractions we describe the experimental data by an interaction model where in a sequence of binary collisions the formation of transient negative ions is the key feature. Comparison of the results for scattering from the two different surfaces reveals that the different electronic structures of the two materials have a pronounced effect on the electronic interactions during the collisions in front of the topmost layer of the surface plane. The lower binding energies of valence band electrons for KI result in substantially higher probabilities for electronic excitations. On the other hand, the electronic structure of KI leads compared to LiF to an additional channel for electron loss, resonant transfer of electrons from the negative ions to the conduction band. This partly compensates the enhanced initial capture probabilities concerning the total electron emission yields and the formation (survival) of negative ions. Our analysis of data in terms of an effective description may lead to a quantitative understanding of the interactions of atoms in front of insulator surfaces. We hope that our work will stimulate theoretical studies on the collision dynamics based on potential energy diagrams for these interesting systems.

The assistance of C. Auth, D. Blauth, and K. Maass in the preparation and running of the experiments is gratefully acknowledged. One of us (HPW) is grateful to the Alexander-von-Humboldt foundation for generous financial support. This work was supported by DFG (Grant No. Wi 1336) and by Austrian FWF.

References

1. M. Kaminsky, *Atomic and Ionic Impact Phenomena on Metal Surfaces* (Springer, Berlin, 1965)
2. K.H. Krebs, Fortschr. Phys. **16**, 419 (1968)
3. M. Vana, F. Aumayr, P. Varga, H.P. Winter, Europhys. Lett. **29**, 55 (1995)
4. P. Stracke, F. Wiegershaus, S. Krischok, V. Kempter, P.A. Zeijlmans van Emmichoven, A. Niehaus, F.J. Garcia de Abajo, Nucl. Instrum. Meth. B **125**, 67 (1997)
5. P.A. Zeijlmans van Emmichoven, A. Niehaus, P. Stracke, F. Wiegershaus, S. Krischok, V. Kempter, A. Arnau, F.J. Garcia de Abajo, M. Penalba, Phys. Rev. B **59**, 10950 (1999)
6. C. Auth, A.G. Borisov, H. Winter, Phys. Rev. Lett. **75**, 2292 (1995)
7. H. Winter, Progr. Surf. Sci. **63**, 177 (2000)
8. A.G. Borisov, V.A. Esaulov, J. Phys.: Condens. Matter **12**, R177 (2000)
9. A.G. Borisov, V. Sidis, Phys. Rev. B **56**, 10628 (1997)
10. A.G. Borisov, V. Sidis, H. Winter, Phys. Rev. Lett. **77**, 1893 (1996)
11. P. Roncin, J. Villette, J.P. Atanas, H. Khemliche, Phys. Rev. Lett. **83**, 864 (1999)
12. H. Winter, S. Lederer, K. Maass, A. Mertens, F. Aumayr, H.P. Winter, J. Phys. B: At. Mol. Opt. Phys. **35**, 3315 (2002)
13. A. Mertens, S. Lederer, K. Maass, H. Winter, J. Stöckl, H.P. Winter, F. Aumayr, Phys. Rev. B **65**, 132410 (2002)
14. A. Mertens, K. Maass, S. Lederer, H. Winter, H. Eder, J. Stöckl, H.P. Winter, F. Aumayr, J. Viefhaus, U. Becker, Nucl. Instr. Meth. B **182**, 23 (2001)
15. H. Winter, A. Mertens, S. Lederer, C. Auth, F. Aumayr, H.P. Winter, Nucl. Instr. Meth. B **212**, 45 (2003)
16. D.S. Gemmell, Rev. Mod. Phys. **46**, 129 (1974)
17. H. Winter, Phys. Rep. **367**, 387 (2002)
18. Y.N. Demkov, Sov. Phys. JETP **18**, 138 (1964)
19. R.E. Johnson, *Atomic and Molecular Collisions* (Plenum Press, New York, 1982), p. 116
20. A.G. Borisov, J.P. Gauyacq, Phys. Rev. B **62**, 4265 (2000)
21. F. Aumayr, G. Lakits, HP. Winter, Appl. Surf. Sci. **63**, 17 (1991)
22. A. Mertens, H. Winter, Phys. Rev. Lett. **85**, 2825 (2000)
23. W.P. O'Brien Jr, J.P. Hernandez, Phys. Rev. B **9**, 3560 (1974)
24. W.H. Strehlow, E.L. Cook, J. Phys. Chem. Ref. Data **2**, 163 (1973)
25. A. Mertens, H. Winter, unpublished